

Stochastic simulation of quantum systems and critical dynamics

T. Schneider, M. Zannetti,* and R. Badii

IBM Zurich Research Laboratory, 8803 Rüschlikon, Switzerland

(Received 20 August 1984)

We propose transformation of the Langevin equation into an eigenvalue problem as the framework of the stochastic simulation of quantum systems. The potential of the method is illustrated by numerical results for the low-lying energy levels of one-particle systems and coupled harmonic oscillators. Another application is the relationship between the dynamics of a d -dimensional system evolving according to the Langevin equation, an associated d -dimensional quantum system, and its $(d+1)$ -dimensional classical counterpart. On this basis we relate the critical dynamics to the static properties of an associated quantum system and its $(d+1)$ -dimensional classical analog. This then leads to equalities and scaling relations between the static and dynamic critical exponents. As a specific example, we treat the time-dependent Ginzburg-Landau model without conservation laws. In the large- n limit, the critical dynamics is traced back to Gaussian (tricritical Lifshitz) behavior of the associated $(d+1)$ -dimensional classical model. The static exponents describing the critical dynamics are determined, however, by the crossover from Lifshitz to Gaussian (tricritical Lifshitz) behavior.

I. INTRODUCTION

Stochastic processes, via Monte Carlo techniques^{1,2} and the Langevin equation,^{3,4} are currently widely used in many areas of physics as a tool for numerical simulations. In these techniques stochastic processes are introduced with the requirement that the associated equilibrium density coincides with the probability density of a quantum or classical system which is to be simulated. The equation of motion of the stochastic process can then be used to calculate expectation values of interest in terms of time averages.

In this paper we present an alternative technique to simulate a quantum system, based on the Langevin equation. A preliminary account was given in Ref. 5. This is achieved by considering the Fokker-Planck equation associated with the Langevin equation. In fact, the Fokker-Planck equation can be reduced to the Schrödinger equation by appropriately choosing the variance of the random force. As a result, a system evolving according to the Langevin equation and specified by its potential energy W , is related to a quantum system with potential energy V , where $V(W)$ is known. Consequently, ground-state properties and the energy spectrum of the quantum system can then be investigated by simulating correlation functions in the stationary Langevin process.

Another interesting aspect of this relationship between the Langevin equation and an associated quantum problem stems from the fact that the variables entering the quantum system are canonically conjugate. Accordingly, the quantum system can be mapped on a $(d+1)$ -dimensional classical model. On this basis, it becomes possible to relate the critical dynamics of a d -dimensional system evolving according to the Langevin equation to the static critical properties of the associated quantum system and in turn to the static critical properties of the corre-

sponding $(d+1)$ -dimensional classical system. This then leads to equalities and scaling relations between the dynamic and static critical exponents of these models.

As a specific example, we consider the n -component Landau-Ginzburg model without conservation laws, and construct the associated $(d+1)$ -dimensional model. It is a highly anisotropic system with complex critical behavior. We study this model in the large- n limit and find a critical surface containing a line of Lifshitz points and a line of tricritical points intersecting at a Lifshitz multicritical point. The approach to dynamic criticality in the d -dimensional system is then related to the static properties of a $(d+1)$ -dimensional system along a special trajectory in the parameter space, which terminates at the Gaussian (Lifshitz tricritical) point. The static and dynamic critical exponents of the d -dimensional model are then related to the static critical exponents of the $(d+1)$ -dimensional system by means of the Lifshitz-to-Gaussian (tricritical Lifshitz) crossover. Accordingly, the critical dynamics of the time-dependent Ginzburg-Landau model without conservation laws, is traced back to Gaussian (tricritical Lifshitz) behavior in the associated $(d+1)$ -dimensional model. The static exponents describing the critical dynamics, however, are determined by the crossover from Lifshitz-to-Gaussian (Lifshitz tricritical) behavior.

The paper is organized as follows. In Sec II we sketch the relationship between the model evolving according to the Langevin equation, the associated quantum system, and its $(d+1)$ -dimensional classical counterpart. Section III is devoted to exploring the potential of simulating quantum systems in terms of the Langevin process. We treat one-particle systems and a linear chain of coupled harmonic oscillators, allowing assessment of the accuracy of the method. The mappings of the critical dynamics of a d -dimensional Langevin process without conservation laws onto the static properties of an associated d -

dimensional quantum model and its $(d+1)$ -dimensional classical counterpart are presented in Sec. IV.

II. BASIC FORMALISM

In this section we sketch the relation between the Langevin-Fokker-Planck and the Schrödinger equations.⁶ This relationship allows estimation of quantum properties from the time evolution of an associated system satisfying the Langevin equation or vice versa. Moreover, it connects the dynamics of a d -dimensional Langevin system with a d -dimensional quantum system which in turn can be mapped on a $(d+1)$ -dimensional classical system. To sketch the method, we first consider a one-particle system with time evolution defined by the stochastic differential equation of the Langevin type

$$\dot{x} = \frac{dx}{dt} = -\frac{\partial W}{\partial x} + \eta(t), \quad (2.1)$$

where η is a Gaussian random force with

$$\langle \eta(t) \rangle = 0, \quad \langle \eta(t)\eta(t') \rangle = \sigma \delta(t-t'). \quad (2.2)$$

The associated Fokker-Planck equation for the probability density is

$$\frac{\partial \rho}{\partial t} = \frac{\partial}{\partial x} \left[\frac{\partial W}{\partial x} \rho \right] + \frac{\sigma}{2} \frac{\partial^2 \rho}{\partial x^2}. \quad (2.3)$$

In the stationary equilibrium state, it admits the time-independent solution

$$\rho_{\text{eq}} \sim e^{-2W/\sigma}. \quad (2.4)$$

By invoking the transformation

$$\rho(x,t) = \rho_{\text{eq}}^{1/2} \Psi(x,t), \quad (2.5)$$

it reduces to

$$-\frac{\partial \Psi}{\partial t} = \left[-\frac{\sigma}{2} \frac{\partial^2 \Psi}{\partial x^2} + V \right] \Psi. \quad (2.6)$$

The potentials W and V are related by the Riccati equation

$$V = \frac{1}{2\sigma} \left[\frac{\partial W}{\partial x} \right]^2 - \frac{1}{2} \frac{\partial^2 W}{\partial x^2}. \quad (2.7)$$

The associated eigenvalue problem,

$$\left[-\frac{\sigma}{2} \frac{\partial^2}{\partial x^2} + V \right] \varphi_m = \lambda_m \varphi_m, \quad (2.8)$$

yields a non-negative energy spectrum, with

$$\lambda_0 = 0, \quad \varphi_0 = \rho_{\text{eq}}^{1/2}. \quad (2.9)$$

The general solution of the Fokker-Planck equation can then be expressed as

$$\rho(x,t) = \varphi_0^2 + \varphi_0 \sum_{m=1}^{\infty} c_m \varphi_m e^{-\lambda_m t}. \quad (2.10)$$

By invoking the initial condition

$$\rho(x,0) = \delta(x-x'), \quad (2.11)$$

and denoting the solution with this initial condition as $\rho(x,t|x')$, we obtain

$$\rho(x,t|x') = \varphi_0(x) \sum_{m=0}^{\infty} \frac{\varphi_m(x')}{\varphi_0(x')} \varphi_m(x) e^{-\lambda_m t}, \quad (2.12)$$

reducing for $t=0$ to Eq. (2.11). Stationary two-time correlation functions can then be expressed as

$$\begin{aligned} \langle x(t)x(0) \rangle &= \int dx \int dx' x x' \rho_{\text{eq}}(x') \rho(x,t|x') \\ &= \sum_m |\langle 0|x|m \rangle|^2 e^{-\lambda_m t}, \end{aligned} \quad (2.13)$$

reducing for $t=0$ to

$$\langle x(0)x(0) \rangle = \langle x^2 \rangle = \int \varphi_0^2 x^2 dx. \quad (2.14)$$

Ergodicity of the Langevin process implies that these quantities can also be obtained from the solution of the Langevin equation (2.1) in terms of time averages, namely,

$$\begin{aligned} \langle x(t)x(0) \rangle &= \lim_{t_n-t_m \rightarrow \infty} \frac{1}{t_n-t_m} \\ &\quad \times \int_{t_m}^{t_n-t} x(t')x(t'+t) dt' \end{aligned} \quad (2.15)$$

and

$$\langle x^2 \rangle = \lim_{t_n-t_m \rightarrow \infty} \frac{1}{t_n-t_m} \int_{t_m}^{t_n} x^2(t') dt'. \quad (2.16)$$

The long-time behavior of the Langevin process then provides estimates for the lowest eigenvalues λ_{m_L} with $\langle 0|x^p|m_L \rangle \neq 0$, from

$$\langle x^p(t)x^p(0) \rangle \xrightarrow{t \rightarrow \infty} |\langle 0|x^p|m_L \rangle|^2 e^{-\lambda_{m_L} t}. \quad (2.17)$$

This set of equations constitutes the framework for the correspondence between a Langevin process and a quantum problem. In fact, considering the Schrödinger equation

$$i \frac{\partial \Psi}{\partial t} = \frac{1}{\hbar} \mathcal{H} \Psi, \quad \mathcal{H} = -\frac{\hbar^2}{2m} \frac{\partial^2}{\partial x^2} + \tilde{V}(x), \quad (2.18)$$

and setting

$$\Psi \sim e^{-i\lambda_m t} \varphi_m(x), \quad (2.19)$$

we obtain the eigenvalue problem

$$\left[-\frac{\hbar}{2m} \frac{\partial^2}{\partial x^2} + \frac{1}{\hbar} \tilde{V}(x) \right] \varphi_m = \lambda_m \varphi_m, \quad (2.20)$$

which is identical to the corresponding Fokker-Planck expressions, Eqs. (2.6) and (2.8), provided that

$$t \rightarrow it, \quad \sigma = \frac{\hbar}{m}, \quad \frac{1}{\hbar} \tilde{V}(x) = V(x). \quad (2.21)$$

From Eqs. (2.13)–(2.17) it then follows that the ground-state properties of this quantum system can be obtained as time averages from the solutions of the Langevin process (2.1).

For the purpose of numerical simulation, this correspondence might be used in two ways.

(i) The potential V entering the quantum problem is constructed from a given W by means of the Riccati equation (2.7).

(ii) For a given V , the potential W entering the Langevin process must be obtained from an independent method of solution of the Schrödinger equation for the ground-state.

In case (ii), W might be obtained by solving the Riccati equation (2.7), which now reads

$$V(x) - \lambda_0 = \frac{1}{2\sigma} \left[\frac{\partial W}{\partial x} \right]^2 - \frac{1}{2} \frac{\partial^2 W}{\partial x^2}. \quad (2.22)$$

In general, λ_0 does not vanish and must be determined from the Schrödinger equation. From the corresponding ground-state wave function W might then also be obtained as

$$W = -\sigma \ln \varphi_0. \quad (2.23)$$

In fact, substitution of this expression into Eq. (2.22) yields the Schrödinger equation. Moreover, the eigenvalues in Eqs. (2.13) and (2.17) must then be replaced by $\lambda_m \rightarrow \tilde{\lambda}_m = \lambda_m - \lambda_0$. The ground-state eigenvalue and eigenfunctions of the quantum problem defined by $V(x)$ are denoted by λ_0 and φ_0 , respectively.

The connection between the Langevin equation and the quantum problem can also be illustrated in terms of the probability distribution over sample paths, allowing a simpler generalization to the case of infinitely many degrees of freedom. From the Feynman-Kac formula, this is given by

$$d\mu_{\text{eq}}[x(t)] \sim \exp \left[- \int_{-\infty}^{+\infty} \left(\frac{\dot{x}^2}{2\sigma} + V(x) \right) dt \right] \mathbf{D}x(t), \quad (2.24)$$

where $\mathbf{D}x(t)$ is the usual formal measure on paths, and $V(x)$ is given by Eq. (2.7). Now, setting $\sigma = \hbar/m$, the above expression is recognized as the probability measure arising in the Euclidean (imaginary time) representation of the ground-state expectations for the quantum problem with potential $V(x)$. Finally, note that Eq. (2.24) can also be interpreted as the Gibbs equilibrium measure of a classical system in one space dimension,⁷ yielding for the partition function the expression

$$Z \sim \int \mathbf{D}x(t) \exp \left[- \int_{-\infty}^{+\infty} \left(\frac{\dot{x}^2}{2\sigma} + V \right) dt \right]. \quad (2.25)$$

The method is easily extended to N -particle systems. The stochastic dynamics without conservation laws is described by a set of coupled Langevin equations, which now read

$$\dot{x}_l = - \frac{\partial W}{\partial x_l} + \eta_l(t). \quad (2.26)$$

The N -independent Gaussian noise sources satisfy

$$\langle \eta_l(t) \rangle = 0, \quad \langle \eta_l(t) \eta_{l'}(t') \rangle = \sigma \delta_{ll'} \delta(t - t'). \quad (2.27)$$

As in the one-particle case, the associated Fokker-Planck equation leads to an eigenvalue problem [Eq. (2.8)], which

now reads

$$\left[- \frac{\sigma}{2} \sum_l \frac{\partial^2}{\partial x_l^2} + V(x_1, \dots, x_n) \right] \varphi_n = \lambda_n \varphi_n, \quad (2.28)$$

where V is given in terms of W by the Riccati equation

$$V = \frac{1}{2\sigma} \sum_l \left[\frac{\partial W}{\partial x_l} \right]^2 - \frac{1}{2} \sum_l \frac{\partial^2 W}{\partial x_l^2}. \quad (2.29)$$

In terms of these eigenfunctions and eigenvalues, correlation functions can be expressed as

$$C(q, t) = \langle x(q, t) x(-q, 0) \rangle = \sum_n | \langle 0 | x(q) | n \rangle |^2 e^{-\lambda_n t}, \quad (2.30)$$

where

$$x(q, t) = \frac{1}{\sqrt{N}} \sum_l e^{iql} [x_l(t) - \langle x_l \rangle]. \quad (2.31)$$

Correlation functions might also be obtained from the solution of the Langevin equations (2.26) in terms of time averages [Eqs. (2.15) and (2.16)],

$$\begin{aligned} \langle x(q, t) x(-q, 0) \rangle &= \lim_{t_n - t - t_m \rightarrow \infty} \frac{1}{t_n - t - t_m} \\ &\times \int_{t_m}^{t_n - t} x(q, t') x(-1, t + t') dt'. \end{aligned} \quad (2.32)$$

The long-time behavior then provides, as in the one-particle case [Eq. (2.17)], estimates for the lowest eigenvalues and the corresponding matrix element.

Following the steps outlined in the one-particle case [Eqs. (2.18)–(2.21)], we obtain from Eq. (2.28) for the Hamiltonian of the associated quantum system the expression

$$\frac{1}{\hbar} \mathcal{H} = - \frac{\hbar}{2m} \sum_l \frac{\partial^2}{\partial x_l^2} + V = \sum_l \frac{m \dot{x}_l^2}{2\hbar} + V \quad (2.33)$$

having the same eigenvalues and eigenfunctions as the Fokker-Planck eigenvalue problem (2.28), provided that $\sigma = \hbar/m$. Accordingly, the ground-state properties of this N -particle quantum system can be obtained from the solution of the Langevin equations (2.26) in terms of time averages.

For the purpose of numerical simulation and in full analogy to the one-particle case, this correspondence can be used in two ways. (i) The potential V entering the quantum problem is constructed from a given W by means of the Riccati equation (2.29). (ii) For a given V , the potential W , entering the Langevin equation, must be obtained from an independent method of solution of the Schrödinger equation, such as the Green's-function Monte Carlo technique, providing the ground-state wave function and eigenvalue of the quantum problem with potential V . With use of Eq. (2.23), W can then be expressed in terms of the ground-state wave function.

The connection between a d -dimensional system evolving according to the Langevin equation, an associated d -

dimensional quantum problem and a corresponding $(d+1)$ -dimensional classical system can be established most conveniently in terms of the probability measure over sample paths,⁷ by the generalization of Eq. (2.24),

$$d\mu_{\text{eq}}[x_i(t)] \sim e^{-S[x_i]} \prod_I \mathbf{D}x_i(t), \quad (2.34)$$

with the action functional

$$S[x_i(t)] = \int_{-\infty}^{+\infty} \frac{1}{\hbar} \mathcal{H} dt = \int_{-\infty}^{+\infty} \sum_I \left[\frac{\dot{x}_I^2}{2\sigma} + V \right] dt, \quad (2.35)$$

where V is given in terms of W by the Riccati equation (2.29). As in the one-particle case, the connection between the Langevin equation and the related quantum problem can be established after setting $\sigma = \hbar/m$ and identifying Eq. (2.34) as the probability measure arising in the Euclidean (imaginary time) representation of ground-state expectations for the quantum system with potential V . Furthermore, by regarding t as a spacelike variable in (2.35), we can treat Eq. (2.34) as the ensemble probability density of a classical $(d+1)$ -dimensional system, provided the system evolving according to the Langevin equations is embedded in d dimensions. Its partition function is

$$Z \sim \int \prod_I \mathbf{D}x_i(t) e^{-S[x_i(t)]}. \quad (2.36)$$

Finally, we quote the corresponding expressions for a system characterized by an n -component field $\phi_\alpha(\underline{x}, t)$, $\alpha = 1, \dots, n$, in d -dimensional space. The Langevin equation then reads

$$\frac{\partial \phi_\alpha(\underline{x}, t)}{\partial t} = - \frac{\delta W[\underline{\phi}]}{\delta \phi_\alpha} + \eta_\alpha(\underline{x}, t). \quad (2.37)$$

$W[\underline{\phi}]$ is a functional of $\underline{\phi}(\underline{x}, t)$ and $\eta_\alpha(\underline{x}, t)$ is a Gaussian noise with

$$\begin{aligned} \langle \eta_\alpha(\underline{x}, t) \rangle &= 0, \\ \langle \eta_\alpha(\underline{x}, t) \eta_\beta(\underline{x}', t') \rangle &= \sigma \delta_{\alpha\beta} \delta(\underline{x} - \underline{x}') \delta(t - t'). \end{aligned} \quad (2.38)$$

The corresponding probability measure over paths [Eq. (2.34)] is now given by

$$d\mu_{\text{eq}}[\underline{\phi}(\underline{x}, t)] \sim e^{-S[\underline{\phi}]} \prod_{\alpha=1}^n \mathbf{D}\phi_\alpha(\underline{x}, t), \quad (2.39)$$

with the action functional

$$\begin{aligned} S[\underline{\phi}] &= \int_{-\infty}^{+\infty} \frac{1}{\hbar} \mathcal{H} dt \\ &= \int_{-\infty}^{+\infty} dt \int d^d x \left[\sum_\alpha \frac{\dot{\phi}_\alpha^2}{2\sigma} + \sum_\alpha V(\phi_\alpha) \right]. \end{aligned} \quad (2.40)$$

The potential V can be expressed in terms of W by the Riccati equation

$$V[\phi_\alpha] = \frac{1}{2\sigma} \left[\frac{\delta W}{\delta \phi_\alpha} \right]^2 - \frac{1}{2} \frac{\delta^2 W}{\delta \phi_\alpha^2}. \quad (2.41)$$

As in the N -particle case, the connection between the system evolving according to the Langevin equation and the quantum model with Hamiltonian \mathcal{H} is established by setting $\sigma = \hbar/m$ and by identifying Eq. (2.40) with the ground-state probability measure in Euclidean quantum-field theory. Furthermore, by considering t as a spacelike variable in Eq. (2.40), we identify expression (2.40) as the ensemble probability density of a classical $(d+1)$ -dimensional system with interaction S .

The formalism outlined in this section might then be used as follows. (i) Ground-state properties of a given quantum system can be simulated in terms of the Langevin process, provided the ground-state wave function and eigenvalue are known. (ii) The long-time behavior of a Langevin process provides information on the ground-state properties of an associated quantum system. (iii) The dynamics of a d -dimensional system evolving according to the Langevin process can be mapped onto an associated d -dimensional quantum system, specified by the Riccati equation (2.29) and with canonically conjugate variables. Such quantum systems do have a $(d+1)$ -dimensional classical analog. Consequently, the critical dynamics of a Langevin process in d dimensions can be related to the static properties of the associated d -dimensional quantum model and its $(d+1)$ -dimensional classical counterpart. These implications will be discussed in detail in the following sections.

III. NUMERICAL SIMULATIONS

In this section we explore the potential of the Langevin approach to simulate quantum systems. To assess the accuracy of the method, we treat some single-particle systems and a chain of harmonic oscillators, where the properties of interest can also be calculated by other techniques. As mentioned above, there are two possible starting points: either the quantum potential $V(x)$ is given, or $W(x)$: In the latter case, a quantum system is defined in terms of the Riccati equation.

A. Simulation of ground-state properties of a given quantum system

In the case of one-particle systems, results can be compared with those obtained by direct integration of the Schrödinger equation or by diagonalization of the Hamiltonian. For many-particle systems, the method requires an independent knowledge of the ground-state eigenfunction and eigenvalue. These properties might be obtained by other techniques.¹

As an example, we treat the quartic quantum oscillator with

$$V(x) = \frac{x^4}{4}. \quad (3.1)$$

φ_0 and λ_0 are readily evaluated by means of standard Runge-Kutta integration of the Schrödinger equation (2.8). The corresponding classical potential

$$W(x) = -\sigma \ln \varphi_0(x), \quad (3.2)$$

was then tabulated for $\sigma = 1$, in order to perform the numerical integration of the Langevin equation (2.1) and to

compute the correlation functions (2.17). All the simulations were performed using the algorithm outlined in Ref. 8. To obtain good statistics, averages were taken over 4000 to 8000 independent runs with integration steps ranging from 0.01 to 0.001. Having reached equilibrium, these trajectories were sampled on a grid with time steps between 0.01 and 0.2 up to 4096 points, to calculate the correlation functions (2.17). The first two energy levels $\lambda_1 - \lambda_0$ and $\lambda_2 \lambda_0$ were then extracted from the long-time behavior of $\langle x(t)x(0) \rangle$ and $\langle x^2(t)x^2(0) \rangle$ (Fig. 1), respectively. A comparison between these results and those obtained by direct integration is given in Table I, where $\lambda_0 = 0.42080$. In Fig. 2 the potentials $V(x)$ and $W(x)$ are displayed, where $W(x)$ was shifted vertically to the origin for ease of comparison. Clearly, $W(x)$ will change by varying $\sigma = \hbar/m$. By keeping \hbar constant and decreasing the mass m , the energy levels of $V(x)$ acquire both a larger separation and higher energies. The effect of σ on the shape of $W(x)$ is to increase its steepness with increasing σ .

B. Simulation of the ground-state properties of a resulting quantum system

Next, we consider two examples where $V(x)$ is derived from a suitable drift potential $W(x)$, by invoking the Riccati equation (2.7). In the first example, $W(x)$ is given by

$$W(x) = \frac{A}{2}x^2 + \frac{B}{4}x^4. \quad (3.3)$$

The resulting $V(x)$ might exhibit a rich structure depending on the choice of parameters A and B . The choice $A = -1$ and $B = 1$ yields a double-well quantum potential where tunnel splitting occurs for σ less than $\sigma_s = 1.2$. In particular, for $\sigma = 1$, the first excited state has the eigenvalue $\lambda_1 = 0.4229$, which is slightly below the maximum of the potential at the origin $V(0) = 0.5$. When σ decreases, we obtain a dense spectrum of split levels below $V(0) = 0.5$. In the opposite case, $\sigma \gg 1$, the quantum fluctuations become so strong that tunnel splittings become suppressed. The σ dependence of the first few energy levels is displayed in Fig. 3.

The two lowest energy levels were estimated from the

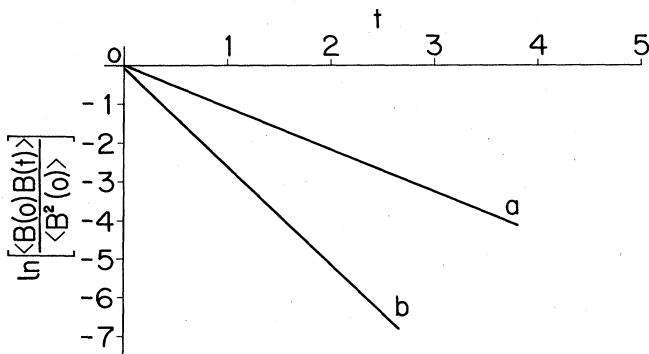


FIG. 1. Time dependence of the correlation function $\ln \langle x^p(t)x^p(0) \rangle / \langle x^p(0)x^p(0) \rangle$ as obtained from the Langevin simulation of the quartic quantum oscillator. Curve a, $p = 1$; curve b, $p = 2$.

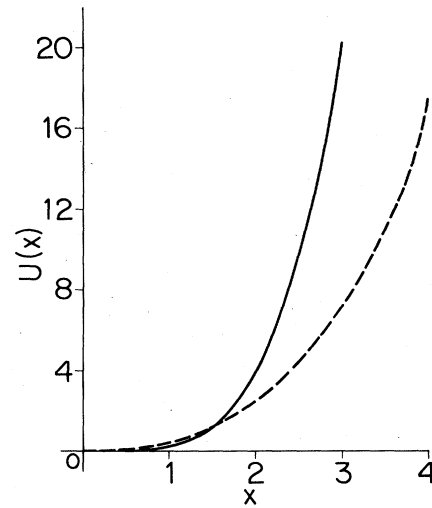


FIG. 2. Comparison between the potential $V(x) = x^4/4$ of the quartic quantum oscillator (solid line) and $W(x)$ [Eq. (2.23)] (dashed line) for $\sigma = 1$.

long-time behavior of $\langle x(t)x(0) \rangle$ and $\langle x^2(t)x^2(0) \rangle$. The results are listed in Table I. For comparison, we again included the corresponding values as obtained from the Runge-Kutta method.

The last single-particle example is defined by

$$W(x) = 1 - \cos x, \quad (3.4)$$

yielding with the Riccati equation (2.7) the potential

$$V(x) = \frac{1}{2\sigma} \sin^2 x - \frac{1}{2} \cos x, \quad (3.5)$$

which is plotted in Fig. 4. This example differs from the previous ones, since there are no bound states. The band

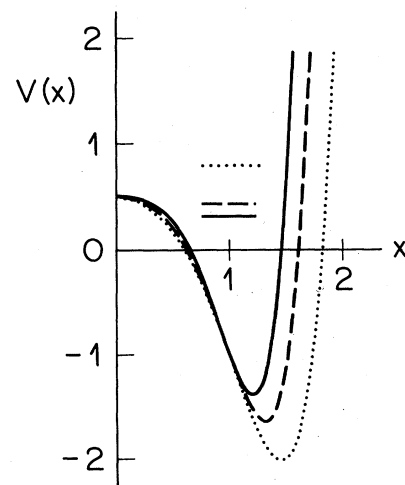


FIG. 3. Potential $V(x)$ resulting from $W(x) = -1/2x^2 + 1/4x^4$ by invoking the Riccati equation (2.7) for various values of σ . Solid line, $\sigma = 0.5$; dashed line, $\sigma = 1$; dotted line, $\sigma = 2$. The first-excited states are displayed by the horizontal segments, with the same convention as for the potentials.

TABLE I. Comparison between the eigenvalues $\lambda_n = \lambda_0$ obtained from the stochastic simulation (L) and other methods for $\sigma=1$. RK denotes Runge-Kutta, and D the diagonalization estimates, respectively. The errors are estimates from linear regression.

| | $V(x) = x^4/4$ | | $W(x) = -x^2/2 + x^4/4$ | | $W(x) = 1 - \cos x$ ($k=0$) | | $W(x) = 1 - \cos x$ ($k = \frac{1}{2}$) | | $W = c \int_{-1}^1 12 \sum_{i=1}^L x_i^2 + \frac{1}{2} \sum_{i=1}^L (x_{i+1} - x_i)^2$ | |
|-------------------------|----------------|-------------|-------------------------|-------------|-------------------------------|-------------|---|--------------|--|-----------|
| | RK | L | RK | L | D | L | D | L | Exact | L |
| $\lambda_1 - \lambda_0$ | 1.0871 | 1.090±0.005 | 0.4229 | 0.422±0.003 | 0.82368 | 0.825±0.005 | 0.010248 | 0.0105±0.002 | 1 | 1.01±0.02 |
| $\lambda_2 - \lambda_0$ | 2.5379 | 2.525±0.005 | 2.3149 | 2.330±0.008 | 0.82368 | 0.825±0.005 | 0.59463 | 0.592±0.005 | 2 | 2.05±0.05 |

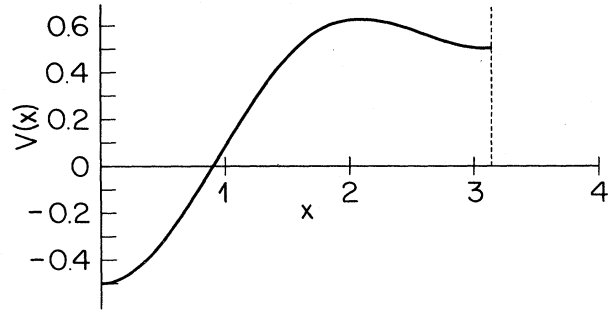


FIG. 4. Potential $W(x) = (1/2\sigma)\sin^2 x - \frac{1}{2}\cos x$ for $\sigma=1$.

structure associated with the potential $V(x)$ can be obtained by diagonalization in a basis of orthogonalized plane waves. In fact,

$$\varphi_n(k) = \sum_g a_{ng}(k) e^{i(k+g)x} \tag{3.6}$$

yields the eigenvalue problem

$$\left[\sigma \frac{(k+g)^2}{2} + V(0) - \omega \right] a_{ng}(k) + \sum_{g' \neq 0} V(g') a_{n,g-g'}(k) = 0, \tag{3.7}$$

where

$$V(g) = \frac{1}{2\pi} \int_0^\pi V(x) \cos(gx) dx, \tag{3.8}$$

and for $\sigma=1$,

$$V(0) = \frac{1}{4}, \quad V(1) = -\frac{1}{4}, \quad V(2) = -\frac{1}{8}. \tag{3.9}$$

The resulting band structure is shown in Fig. 5. It is

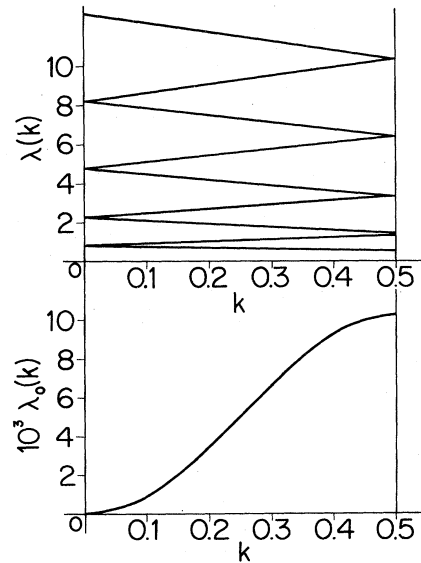


FIG. 5. Band structure associated with the potential $V(x)$ given by Eq. (3.5) for $\sigma=1$. Note that the gaps are appreciable only between the first and second as well as the third and fourth bands.

readily seen that the gaps are very small except the ones between the first and second, as well as the third and fourth energy levels.

From the diagonalization, it is also possible to evaluate correlation functions of the form $\langle \sin[qx(t)]\sin[qx(0)] \rangle$. For $q=1$, we obtain

$$\langle \sin x(t)\sin x(0) \rangle = \sum_n c_n^2(k=1)e^{-\lambda_n(k=0)t}, \quad (3.10)$$

where

$$c_n^2(k=0) = \frac{1}{4} \left| \sum_g a_{0g}(k=0)a_{n,g-1}(k=0) + \sum_g a_{0g}(k=0)a_{n,g+1}(k=0) \right|^2. \quad (3.11)$$

These coefficients and the corresponding eigenvalues are listed in Table II. It is evident that the contribution of higher eigenvalues is negligible after a rather short time, giving an indication of the sampling time required and of the precision attainable in the stochastic simulation. By varying q from $\frac{1}{2} \leq q \leq 1$, it is possible to estimate the lowest bands from $0 \leq k \leq 1$ from the long-time behavior of the correlation functions. In fact the lowest two energy levels at $k=0$ are obtained from $\langle \sin x(t)\sin x(0) \rangle$ and $\langle \cos x(t)\cos x(0) \rangle$, respectively, while those at $k=\frac{1}{2}$ follow from

$$\langle \cos \frac{1}{2}x(t)\cos \frac{1}{2}x(0) \rangle$$

and

$$\langle \sin \frac{1}{2}x(t)\sin \frac{1}{2}x(0) \rangle.$$

The corresponding estimates as obtained from the simulation are listed in Table I, where we also included the results from the diagonalization to assess the accuracy.

When σ is decreased, more energy gaps appear and accordingly more energy bands are in the wells of the potential. Hence, we recover the classical regime where the particle is localized in a well. For large σ , however, the quantum fluctuations become very strong, the particle is no longer affected by the details of the potential, behaving as nearly free.

C. Extension to N -particle systems

As an example of a many-particle system we treat a one-dimensional chain of coupled harmonic oscillators. W

TABLE II. Eigenvalues λ_n ($K=0$) of the potential $V(x)$ [Eq. (3.5)] for $\sigma=1$ and the associated coefficients C_n of the correlation function Eq. (3.10). Note that the contributions of the higher-energy levels become negligibly small after a rather short time.

| n | C_n | λ_n |
|-----|--------------|-------------|
| 1 | -0.30 | 0.823 683 |
| 2 | -0.48 | 0.823 683 |
| 3 | 0.11 | 2.270 294 |
| 4 | -0.11 | 2.270 294 |
| 5 | 0.02 . . . | 4.758 789 |
| 6 | -0.02 . . . | 4.758 789 |
| 7 | 0.001 . . . | 8.254 921 |
| 8 | -0.001 . . . | 8.254 921 |

is defined by

$$W = \frac{A}{2} \sum_l x_l^2 + \frac{C}{2} \sum_l (x_{l+1} - x_l)^2, \quad (3.12)$$

yielding the Langevin equation

$$\dot{x}_l = -Ax_l - C(2x_l - x_{l+1} - x_{l-1}) + \eta_l(t). \quad (3.13)$$

With the transformation (2.31), the Langevin equation reduces to

$$\dot{x}(q,t) = -\omega(q)x(q,t) + \eta(q,t), \quad (3.14)$$

where

$$\omega(q) = A = 2C(1 - \cos q). \quad (3.15)$$

The eigenvalues of the associated quantum problem (2.28) are readily determined. The result is the spectrum of the harmonic chain

$$\lambda_n(q) = n\omega(q), \quad n=0,1,2,\dots \quad (3.16)$$

without the zero-point energy.

Extraction of the quantum properties from the correlation functions of the stochastic process proceeds as in the one-particle case. The simulation was performed with 24 independent chains composed of 500 oscillators each. Results are again listed in Table I, for $A=1$, $C=1$, and $\sigma=1$, evaluated for $q=0$. As expected, the statistics is worse than in the one-particle cases, but still satisfactory.

From the results presented here and summarized in Table I, it is evident that the stochastic approach allows rather accurate estimates of the eigenvalues of an associated quantum system. Clearly, it is only limited by the length of the integration step, the number of independent systems and the number of sampling steps. To disentangle the contribution of the lowest eigenvalue in the decay of a correlation function, it is necessary to choose the sampling time appropriately. Moreover, algorithms have been developed to disentangle several exponentially decaying terms by means of the Padé-Laplace method.⁹

IV. MAPPING OF THE CRITICAL DYNAMICS ONTO THE STATIC PROPERTIES OF AN ASSOCIATED $(d+1)$ -DIMENSIONAL MODEL

In Sec. II we have mapped the dynamics of a d -dimensional system evolving according to the Langevin process (2.26) onto an associated d -dimensional quantum system with canonically conjugate variables. As indicated there, such quantum systems do have a $(d+1)$ -dimensional classical analog. This relationship implies that the critical dynamics of a d -dimensional Langevin process is related to the static critical properties of an associated $(d+1)$ -dimensional classical system.

In this section we derive an exact relation between static and dynamic critical exponents. Invoking then the dynamic scaling hypothesis, we obtain various scaling relations between the critical exponents of the associated models. Finally, we explore the interpretation of the dynamic critical properties in terms of the statics of the underlying $(d+1)$ -dimensional model by using the $1/n$ expansion.

A. Exact relation between dynamic and static critical exponents

We assume that our model W evolving according to the Langevin equation (2.37) exhibits critical slowing down of the order-parameter fluctuations, characterized by^{10,11}

$$\int_0^\infty C_W(\mathbf{q}=\mathbf{0}, t) dt \sim \left| \frac{r_0 - r_{0c}}{r_{0c}} \right|^{-(\Delta_W + \gamma_W)}, \quad (4.1)$$

where

$$C_W(\mathbf{q}, t) = \langle \phi_\alpha(\mathbf{q}, t) \phi_\alpha(-\mathbf{q}, 0) \rangle, \quad (4.2)$$

$$\phi_\alpha(\mathbf{q}, t) = \int d^d x e^{i\mathbf{q}\cdot\mathbf{x}} [\phi_\alpha(\mathbf{x}, t) - \langle \phi_\alpha \rangle].$$

It is understood that σ is fixed and the critical point r_{0c} is reached by varying r_0 . γ_W denotes the exponent of the equal-time correlation function

$$C_W(\mathbf{q}=\mathbf{0}, t=0) \sim \left| \frac{r_0 - r_{0c}}{r_{0c}} \right|^{-\gamma_W} \quad (4.3)$$

of model W . Δ_W is the dynamic critical exponent characterizing the slowing down of the order-parameter fluctuations. As shown in Sec. II [Eq. (2.40)], the Langevin equation (2.37) is associated with a d -dimensional quantum model defined by

$$\mathcal{H} = \int d^d x \left[\sum_\alpha \frac{\dot{\phi}_\alpha^2}{2\sigma} + V[\phi_\alpha] \right], \quad (4.4)$$

where V is given in terms of W by the Riccati equation (2.41). The time integral of the correlation function $C_W(\mathbf{q}=\mathbf{0}, t)$ [Eq. (4.1)] and the zero-frequency susceptibility of the quantum system are then related by

$$\begin{aligned} \int_0^\infty C_W(\mathbf{q}=\mathbf{0}, t) dt &= \sum_n \frac{(\langle 0 | \phi_\alpha(\mathbf{q}=\mathbf{0}) | n \rangle)^2}{\lambda_n} \\ &= \frac{1}{2} \chi_{\mathcal{H}}(\mathbf{q}=\mathbf{0}, \omega=0). \end{aligned} \quad (4.5)$$

$\chi_{\mathcal{H}}(\mathbf{q}, \omega)$ is the wave-vector- and frequency-dependent zero-temperature susceptibility of the associated quantum model \mathcal{H} . At criticality r_{0c} , $\chi_{\mathcal{H}}(0, 0)$ diverges as

$$\chi_{\mathcal{H}}(\mathbf{q}=\mathbf{0}, \omega=0) \sim \left| \frac{r_0 - r_{0c}}{r_{0c}} \right|^{-\gamma_{\mathcal{H}}}. \quad (4.6)$$

Combining then Eqs. (4.1), (4.5), and (4.6), we obtain the exponent equality

$$\Delta_W + \gamma_W = \gamma_{\mathcal{H}}. \quad (4.7)$$

Finally, from Eq. (2.39) we know that the d -dimensional quantum model \mathcal{H} does have a $(d+1)$ -dimensional classical analog with identical critical behavior. Its susceptibility or equal-time correlation function behaves at criticality r_{0c} as

$$C_S \sim \chi_S \sim \left| \frac{r_0 - r_{0c}}{r_{0c}} \right|^{-\gamma_S}. \quad (4.8)$$

Accordingly,

$$\Delta_W + \gamma_W = \gamma_{\mathcal{H}} = \gamma_S. \quad (4.9)$$

Hence, the dynamic critical exponent Δ_W is traced back to the static susceptibility exponents of the associated quantum model and its $(d+1)$ -dimensional classical counterpart, S .

Invoking the lower bound¹²

$$\Delta_W \geq \gamma_W, \quad (4.10)$$

we obtain the inequality

$$\gamma_{\mathcal{H}} = \gamma_S \geq 2\gamma_W. \quad (4.11)$$

These mappings also imply that the dynamic form factor

$$C_W(\mathbf{q}, \omega) = \int dt e^{-i\omega t} C_W(\mathbf{q}, t), \quad (4.12)$$

where $C_W(\mathbf{q}, t)$ is defined in Eq. (4.2), is identical to the equal-time correlation function in our $(d+1)$ -dimensional model S , where the frequency ω plays the role of an additional component $(d+1)$ of the wave vector. Hence,

$$C_W(\mathbf{q}, \omega) = C_S(\mathbf{q}, \omega). \quad (4.13)$$

Moreover, the fluctuation-dissipation theorem implies

$$\chi_S(\mathbf{q}, \omega) \sim C_S(\mathbf{q}, \omega). \quad (4.14)$$

B. Scaling relations

Next, we invoke static and dynamic scaling to derive additional relations between static and dynamic critical exponents. Dynamic scaling implies^{11,13}

$$C_W(\mathbf{q}, \omega) = \xi_W^{2-\eta_W+z_W} f(\xi_W \mathbf{q}, \xi_W^z \omega). \quad (4.15)$$

Integrating over ω and using Eq. (4.1), the usual static scaling law¹³

$$\gamma_W = \nu u_W (2 - \eta_W) \quad (4.16)$$

is recovered.

Turning to our $(d+1)$ -dimensional model S , and introducing the correlation length ξ_{\parallel} in the d -dimensional layers and ξ_{\perp} in the remaining $d+1$ direction, we have from anisotropic scaling

$$\chi_S(\mathbf{q}, \omega) = \xi_{\parallel}^{4-\eta_{\parallel}} \chi_S(\xi_{\parallel} \mathbf{q}, \xi_{\perp} \omega) \quad (4.17)$$

and

$$\chi_S(\mathbf{q}, \omega) = \xi_{\perp}^{2-\eta_{\perp}} \chi_S(\xi_{\parallel} \mathbf{q}, \xi_{\perp} \omega). \quad (4.18)$$

From Eqs. (4.14), (4.15), and (4.17), it then follows that

$$\xi_{\parallel} = \xi_W, \quad \xi_{\perp} = \xi_W^z, \quad (4.19)$$

yielding the following relations between the exponents:

$$\nu_{\parallel} = \nu_W, \quad (4.20a)$$

$$z_W = 2 + \eta_W - \eta_{\parallel} = \frac{4 - \eta_{\parallel}}{2 - \eta_{\perp}} = \frac{\nu_{\perp}}{\nu_{\parallel}}, \quad (4.20b)$$

and

$$\Delta_W = \nu_{\perp}, \quad (4.20c)$$

where

$$\Delta_W = v_W z_W. \quad (4.20d)$$

Furthermore, from Eqs. (4.13), (4.14), (4.17), and (4.18) we have

$$\gamma_S = v_{\parallel}(4 - \eta_{\parallel}) = v_{\perp}(2 - \eta_{\perp}), \quad (4.21)$$

implying with Eqs. (4.20a) and (4.20b)

$$\gamma_S = v_W(2 + z_W - \eta_W). \quad (4.22)$$

C. Dynamics from statics

In this subsection we consider as a specific example for a model W , the n -component Landau-Ginzburg-Wilson functional. The associated $(d+1)$ -dimensional model S is then constructed by the Riccati equation (2.41). This leads to a set of relations among the coupling constants of a more general $d+1$ model, generating a trajectory in the parameter space of the embedding model. To unravel the connection between the critical properties of the embedding model and the Riccati trajectory, characterizing the critical dynamics, we perform $1/n$ calculations to lowest order.

For the W entering the Langevin equation (2.37), we consider the Landau-Ginzburg-Wilson functional

$$W[\phi_{\alpha}] = \int d^d x \left[\frac{r_0}{2} \phi^2 + \frac{g}{4} (\phi^2)^2 + \frac{1}{2} (\nabla \phi)^2 \right], \quad (4.23)$$

where

$$\phi^2 = \sum_{\alpha} \phi_{\alpha}^2, \quad (\nabla \phi)^2 = \sum_{\alpha} (\nabla \phi_{\alpha})^2, \quad \alpha = 1, \dots, n, \quad g = \bar{g}/n. \quad (4.24)$$

Using Eq. (2.40) and the constraints imposed by the Riccati equation (2.41), we obtain in the large- n limit the effective expression

$$2\sigma \tilde{S}[\phi_{\alpha}] = \int dt \int d^d x \left[\left| \frac{\partial \phi}{\partial t} \right|^2 + b \phi^2 + u_4 (\phi^2)^2 + u_6 (\phi^2)^3 + (\nabla^2 \phi)^2 + a \sum_{\alpha} \phi_{\alpha} \nabla^2 \phi_{\alpha} + v \phi^2 \sum_{\alpha} \phi_{\alpha} \nabla^2 \phi_{\alpha} + c \phi^2 \right] \quad (4.30)$$

defining the \tilde{S} model.

The Riccati equation (2.41) imposes the following constraints on the coupling constants, which define the model S , containing the information on the critical dynamics of the W system:

$$\begin{aligned} b &= r_0^2 - 2g\sigma, \quad a = -2r_0, \\ u_4 &= 2r_0g, \quad v = -2g, \\ u_6 &= g^2, \quad c = -g\sigma n. \end{aligned} \quad (4.31)$$

Accordingly, the S system, containing the information on the critical dynamics, can be viewed as a special trajectory defined by the Riccati constraints (4.31) in the parameter space of the \tilde{S} system [Eq. (4.30)]. This model is expected to exhibit a rich variety of critical behavior for general values of the coupling constants. In any case, the dynamics of model W is determined by the point where the Riccati trajectory (4.31) intersects the critical surface of the general model \tilde{S} . To elucidate the physical nature of this

$$\begin{aligned} 2S\sigma &= \sum_{q,\alpha} \int dt \left[\left| \frac{\partial \phi_{\alpha}(\mathbf{q},t)}{\partial t} \right|^2 \right. \\ &\quad \left. + (r_0 + \bar{g} \langle \phi_{\alpha}^2 \rangle + q^2)^2 |\phi_{\alpha}(\mathbf{q},t)|^2 \right] \\ &\quad - \sigma \sum_{q,\alpha} (r_0 + \bar{g} \langle \phi_{\alpha}^2 \rangle + q^2) \end{aligned} \quad (4.25)$$

for the associated $(d+1)$ -dimensional model S . The inverse susceptibility is

$$\chi_S^{-1}(\mathbf{q},\omega) = \omega^2 + (r_0 + \bar{g} \langle \phi_{\alpha}^2 \rangle + q^2)^2, \quad (4.26)$$

where $\langle \phi_{\alpha}^2 \rangle$ must be determined self-consistently from

$$\langle \phi_{\alpha}^2 \rangle = \sum_q \sum_{\omega} \frac{\sigma}{\omega^2 + (r_0 + \bar{g} \langle \phi_{\alpha}^2 \rangle + q^2)^2}. \quad (4.27)$$

From the last two equations and the scaling relations (4.17)–(4.20), the exponents of interest are readily determined. The results are

$$\gamma_S = 2\gamma_W = \begin{cases} 2, & d > 4 \\ \frac{4}{d-2}, & 2 < d < 4 \end{cases} \quad (4.28)$$

and

$$\begin{aligned} \Delta_W &= 2, \quad z_W = 2 \\ \eta_{\perp} &= 0, \quad \eta_{\parallel} = 0. \end{aligned} \quad (4.29)$$

As expected, in the large- n limit we recover $z_W = 2$, corresponding to the prediction of the conventional or Van Hove theory of slowing down.¹¹

For general values of the coupling constants, Eqs. (2.40), (2.41), and (4.23) lead to the expression

intersection, we apply the renormalization group to the model \tilde{S} . In the neighborhood of the Gaussian fixed point, we obtain the scaling relations

$$\begin{aligned} a' &= L^2 a, \quad b' = L^4 b, \quad u_4' = L^{6-d} u_4, \\ u_6' &= L^{2(4-d)} u_6, \quad v' = L^{4-d} v, \quad \sigma' = \sigma L^d, \end{aligned} \quad (4.32)$$

yielding the upper critical dimension $d^* = 6$. This result differs from $d^* = 4$, as obtained from the large- n limit (4.28), or from the renormalization-group approach applied to the Langevin dynamics of our model W .¹¹ This discrepancy suggests that the Riccati trajectory must exhibit multicritical behavior, reducing the upper critical dimension to four. Next, we investigate this possibility in the large- n limit.

In the large- n limit the inverse susceptibility for \tilde{S} is

$$\chi_{\tilde{S}}^{-1}(\mathbf{q},\omega) = \omega^2 + q^4 + \mu_L q^2 + r, \quad (4.33)$$

where r obeys the relation

$$r = \mu_1 + \mu_2 r^{d-2/4} + \mu_3 r^{d-2/2}. \tag{4.34}$$

The coefficients μ_L , μ_1 , μ_2 , and μ_3 are essentially the linear scaling fields in the neighborhood of the Gaussian fixed point, with the scaling properties

$$\begin{aligned} \mu'_i &= L^{\gamma_i} \mu_i, \quad i=L,1,2,3 \\ \gamma_L &= 2, \quad \gamma_1=4, \quad \gamma_2=6-d, \quad \gamma_3=2(4-d). \end{aligned} \tag{4.35}$$

Setting $\mu_1=0$ one obtains the transition surface. On this surface, the transition is second order for $\mu_2>0$ (critical surface) and first order for $\mu_2<0$. Furthermore, on the critical surface there is a line of Lifshitz points¹⁴ for $\mu_L=0$, issuing from the Gaussian fixed point [Lifshitz tricritical point (LTP)] as illustrated in Fig. 6. For $d < 6$, the Gaussian fixed point is unstable and the critical behavior of the Lifshitz line is dominated by the nontrivial Lifshitz fixed point (LP). Finally, the phase diagram is completed by the $\mu_2=0$ line, separating the critical surface from the first-order region. For $d > 4$, this is a line of tricritical points, dominated by the Gaussian fixed point. The point of intersection between the tricritical and the Lifshitz line, is accordingly a Lifshitz tricritical point. For $d < 4$, one would expect from Eq. (4.35) the branching from the Gaussian to a nontrivial tricritical fixed point, which in the large- n limit, is expected to be unstable for $d < 4$.^{15,16}

From Eq. (4.34), we obtain for the Lifshitz susceptibility exponent

$$\gamma_L = \begin{cases} 1, & d > 6 \\ 4/d - 2, & 2 < d < 6 \end{cases} \tag{4.36}$$

and

$$\gamma_G = \gamma_{LT} = 1 \tag{4.37}$$

at the Gaussian fixed point (Lifshitz tricritical point).

In terms of the linear scaling fields μ , the Riccati constraints (4.31) take the form

$$\mu_L \sim r_0 - r_{0c}, \quad \mu_1 \sim (r_0 - r_{0c})^2, \quad \mu_2 \sim (r_0 - r_{0c}), \tag{4.38}$$

while μ_3 has some finite value. Thus, as r goes to r_{0c} , the Riccati trajectory approaches the critical surface at the Gaussian (or Lifshitz tricritical) point along the direction characterized by

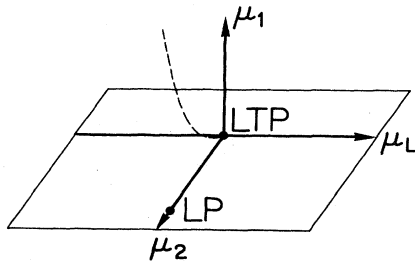


FIG. 6. The plane represents the critical surface of our model \tilde{S} , where the μ_L axis ($\mu_2=0$) is the line of tricritical points, and the μ_2 axis ($\mu_L=0$) that of Lifshitz points. LT denotes the Gaussian (Lifshitz tricritical) fixed point, and LP the Lifshitz fixed point. The dashed line is the Riccati trajectory.

$$\mu_1 \sim \mu_2^2. \tag{4.39}$$

Now, μ_2 is the crossover parameter (along the Lifshitz line) between the Gaussian (Lifshitz tricritical) and the ordinary Lifshitz fixed points (LP) (see Fig. 6). In the neighborhood of the Gaussian point, the crossover of the susceptibility is given by^{17,18}

$$\chi(\mu_1, \mu_2) \sim \mu_1^{-\gamma_G} [f(C)]^{1/\phi}, \tag{4.40}$$

where

$$C = \frac{\mu_2}{\mu_1^\phi}. \tag{4.41}$$

From Eq. (4.35), we obtain for the crossover exponent

$$\phi = \frac{\gamma_2}{\gamma_1} = \frac{6-d}{4} \tag{4.42}$$

and

$$f(c) \sim \begin{cases} 1, & C \ll 1 \\ C^{1/(1-\phi)}, & C \gg 1. \end{cases} \tag{4.43}$$

Along the trajectory given by Eq. (4.39) we have, as $\mu_2 \rightarrow 0$,

$$C \ll 1 \text{ for } d > 4, \tag{4.44}$$

$$C \gg 1 \text{ for } d < 4. \tag{4.45}$$

Accordingly, along this trajectory, the crossover from Gaussian (Lifshitz tricritical) to non-Gaussian behavior occurs at $d = 4$, yielding

$$r \sim \mu_1^{\gamma_G} \sim \mu_2^{2\gamma_G} \sim \mu_2^{\gamma_S}, \tag{4.46}$$

with

$$\gamma_S = 2\gamma_G = 2\gamma_{LT} \text{ for } d > 4, \tag{4.47}$$

in agreement with Eq. (4.28).

In view of the expected instability of the nontrivial Lifshitz tricritical point for $d < 4$, we assume that also for $d < 4$ the behavior along the Riccati trajectory is determined by the Gaussian-to-Lifshitz crossover. Since now $C \gg 1$, we obtain from Eqs. (4.39), (4.40), (4.42), and (4.43),

$$\gamma_S = 2\gamma_L - \frac{\gamma_L - \gamma_G}{\phi}, \tag{4.48}$$

substitution of the large- n limit values for γ_L and γ_G [Eqs. (4.36) and (4.37)] yields

$$\gamma_S = 2\gamma_W = \frac{4}{d-2} \text{ for } d < 4, \tag{4.49}$$

in agreement with the result obtained from the large- n limit of our model S (4.28).

These results then show that the static and the dynamic exponents of our model W can be obtained in terms of the crossover from Lifshitz-to-Gaussian (tricritical Lifshitz) behavior in $d + 1$ dimensions along the Riccati trajectory. The connection between dynamic critical behavior and static critical properties at a Lifshitz point in higher dimensions has also been suggested in the context of the

two-dimensional one-spin-flip Ising model.¹⁹ Our analysis indicates, however, that this issue is rather delicate. In fact, to obtain the correct upper critical dimension, the above-mentioned crossover turns out to be crucial. This we have verified in the large- n limit, where the exponent η vanishes. It would be very interesting to tackle the more general and complicated problem by performing a renormalization-group study of our model \tilde{S} to elucidate further the nature of the Riccati trajectory in the language

of static critical phenomena.

Finally, we note that the method presented here can be extended to stochastic models where the energy, the order parameter, or both, are conserved.²⁰

ACKNOWLEDGMENTS

We acknowledge helpful and clarifying discussions with A. Aharony and H. R. Jauslin.

*Permanent address: Dipartimento di Fisica, Università di Salerno, 84100 Salerno, Italy.

¹D. M. Ceperley and M. H. Kalos, in *Monte Carlo Methods in Statistical Physics*, edited by K. Binder (Springer, Heidelberg, 1979).

²M. Creutz and B. Freedman, *Ann. Phys. (N.Y.)* **132**, 427 (1981).

³G. Parisi and Y. S. Wu, *Sci. Sin.* **24**, 483 (1981).

⁴J. R. Klauder, *Phys. Rev. A* **29**, 2036 (1984).

⁵T. Schneider, M. Zannetti, R. Badii, and H. R. Jauslin (unpublished).

⁶See, for example, N. G. van Kampen, *J. Stat. Phys.* **17**, 71 (1977).

⁷J. B. Kogut, *Rev. Mod. Phys.* **51**, 659 (1979).

⁸R. Morf and E. Stoll, in *Numerical Analysis*, edited by J. Descloux and J. Marti (Birkhauser, Basel, 1977), Vol. 37, p. 139.

⁹A. N. Tikhonov and V. Y. Arsenin, *Solution of Ill-Posed Prob-*

lems (Wiley, New York, 1977).

¹⁰E. Stoll, K. Binder, and T. Schneider, *Phys. Rev. B* **8**, 3266 (1973).

¹¹B. I. Halperin, P. C. Hohenberg, and S. Ma, *Phys. Rev. B* **10**, 139 (1979).

¹²T. Schneider, *Phys. Rev. B* **9**, 3819 (1974).

¹³S. K. Ma, *Modern Theory of Critical Phenomena* (Benjamin, Reading, Mass., 1976).

¹⁴R. M. Hornreich, M. Luban, and S. Shtrikman, *Phys. Rev. Lett.* **35**, (1975).

¹⁵V. Emery, *Phys. Rev. B* **11**, 3397 (1975).

¹⁶S. Sarbach and T. Schneider, *Phys. Rev. B* **16**, 347 (1977).

¹⁷E. K. Riedel and F. Wegner, *Phys. Rev. B* **9**, 294 (1974).

¹⁸M. Zannetti and C. Di Castro, *J. Phys. A* **10**, 1175 (1977).

¹⁹E. Domany, *Phys. Rev. Lett.* **52**, 871 (1984).

²⁰T. Schneider and R. Badii (unpublished).